

Stochastic Flow Models with Delays and Applications to Multi-Intersection Traffic Light Control [★]

Rui Chen ^{*} Christos G. Cassandras ^{*}

^{*} *Division of Systems Engineering, Boston University, Brookline, MA, USA,
(e-mail: ruic@bu.edu, cgc@bu.edu).*

Abstract: We extend Stochastic Flow Models (SFMs), used for a large class of discrete event and hybrid systems, by including the delays which typically arise in flow movement. We apply this framework to the multi-intersection traffic light control problem by including transit delays for vehicles moving from one intersection to the next. Using Infinitesimal Perturbation Analysis (IPA) for this SFM with delays, we derive new on-line gradient estimates of several congestion cost metrics with respect to the controllable green and red cycle lengths. The IPA estimators are used to iteratively adjust light cycle lengths to improve performance and, in conjunction with a standard gradient-based algorithm, to obtain optimal values which adapt to changing traffic conditions. We introduce two new cost metrics to better capture congestion and show that the inclusion of delays in our analysis leads to improved performance relative to models that ignore delays.

Keywords: Performance evaluation, optimization; discrete approaches for hybrid systems; applications;

1 INTRODUCTION

Stochastic Flow Models (SFMs) capture the dynamic behavior of a large class of hybrid systems (see Cassandras and Lafortune [2009]). In addition, they are used as abstractions of Discrete Event Systems (DES), for example when discrete entities accessing resources are treated as flows. The basic building block in a SFM is a queue (buffer) whose fluid content is dependent on incoming and outgoing flows which may be controllable. By connecting such building blocks together, one can generate stochastic flow networks which are encountered in application areas such as manufacturing systems (Armony et al. [2015]), chemical processes (Yin et al. [2013]), water resources (Anderson et al. [2015]), communication networks (Cassandras et al. [2002]) and transportation systems (Geng and Cassandras [2015]). Figure 2 shows a two-node SFM, in which an on-off switch controls the outgoing flow for each node. When the switch at the output of node 1 is turned on, a “flow burst” is generated to join the downstream node 2. Flow models commonly assume that this flow burst can instantaneously join the downstream queue, thus ignoring potentially significant delays before this can happen. Incorporating such delays through more accurate modeling is challenging but crucial in better evaluating the performance of the underlying system and seeking ways to improve it.

Control mechanisms used in SFMs often involve gradient-based methods in which the controller uses estimates of the performance metric sensitivities with respect to controllable parameters in order to adjust the values of these parameters and improve (ideally, optimize) performance. Infinitesimal Perturbation Analysis (IPA) is a method of general applicability to stochastic hybrid systems (see Cassandras et al. [2010], Wardi

et al. [2010]) through which gradients of performance measures may be estimated with respect to several controllable parameters based on directly observable data. The applications of IPA and its advantages have been reported elsewhere (e.g., Cassandras et al. [2010], Fleck et al. [2016]) and are summarized here as follows: (i) IPA estimates have been shown to be unbiased under very mild conditions (Cassandras et al. [2010]). (ii) IPA estimators are robust with respect to the stochastic processes involved. (iii) IPA is event-driven, hence scalable in the number of events in the system, not the (much larger) state space dimensionality. (iv) IPA possesses a decomposability property (Yao and Cassandras [2011]), i.e., IPA state derivatives become memoryless after certain events take place. (v) The IPA methodology can be easily implemented on line, allowing us to take advantage of directly observed data.

While IPA has been extensively used in SFMs, the effect of delays between adjacent nodes, as described above, has not been studied to date. Thus, the contribution of this paper is to incorporate delays in the flow bursts that are created by on-off switching control (see Fig. 2) into the standard SFM and to develop the necessary extensions to IPA for such systems. In addition, an application of SFMs with delays to the Traffic Light Control (TLC) problem in transportation networks is included.

The rest of the paper is organized as follows. In Section 2, we extend the standard multi-node SFM to include delays. In Section 3 we adapt this model to the TLC problem by explicitly modeling the delay experienced by vehicles moving from one intersection to the next. This allows us to introduce two new cost metrics for congestion that incorporate the effect of delays. In Section 4, we carry out IPA for the TLC problem and in Section 5 we provide simulation examples comparing performance results between a model considering traffic delays

^{*} Supported in part by NSF under grants ECCS-1509084, CNS-1645681, and IIP-1430145, by AFOSR under grant FA9550-15-1-0471, by the DOE under grant DE-AR0000796, by the MathWorks and by Bosch.

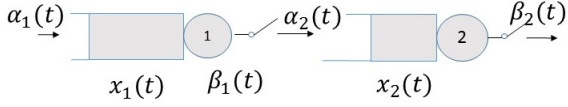


Fig. 1. A two-node SFM.

and one which does not, showing that the former achieves improved performance.

2 STOCHASTIC FLOW MODELS WITH DELAYS

Consider a two-node SFM as in Fig. 2 and let $\{\alpha_i(t)\}$ and $\{\beta_i(t)\}$, $i = 1, 2$, be the *incoming flow* and *outgoing flow processes* respectively. We emphasize that these are both treated as random processes. We define $x(t) = [x_1(t), x_2(t)]$, where $x_i(t) \in \mathbb{R}^+$ is the flow content of node i (we assume that all variables are left-continuous.) The dynamics of this SFM are

$$\dot{x}_i(t) = \begin{cases} 0 & \text{if } x_i(t) = 0, \alpha_i(t) \leq \beta_i(t) \\ & \text{or } x_i(t) = c_i, \alpha_i(t) \geq \beta_i(t) \\ \alpha_i(t) - \beta_i(t) & \text{otherwise} \end{cases} \quad (1)$$

where c_i is the content capacity of i and $\beta_i(t)$ is

$$\beta_i(t) = \begin{cases} h_i(t) & \text{if } G_i(t) = 1 \\ 0 & \text{otherwise} \end{cases} \quad (2)$$

in which $h_i(t)$ is the instantaneous outgoing flow rate at node i , and $G_i(t) \in \{0, 1\}$, $i = 1, 2$ is a switching controller. We also define a clock state variable $z_i(t)$ for each switching controller $G_i(t)$:

$$\dot{z}_i(t) = \begin{cases} 1 & \text{if } G_i(t) = 1 \\ 0 & \text{otherwise} \end{cases} \quad (3)$$

$$z_i(t^+) = 0 \quad \text{if } G_i(t) = 1 \text{ and } G_i(t^+) = 0$$

Thus, when $G_1(t) = 1$, $t \in [t_1, t_2]$, $G_1(t_1^-) = 0$, a flow burst is created at node 1 (when $x_1(t_1) > 0$). In general, several such flow bursts may be created over $(t_1, t_2]$, depending on the values of $\alpha_1(t)$, $h_1(t)$, $t \in (t_1, t_2]$. In SFMs studied to date, we ignore the delay incurred by any such flow burst being transferred between nodes and assume that it instantaneously joins the queue at node 2. Under this assumption,

$$\alpha_2(t) = \begin{cases} \alpha_1(t) & \text{if } x_1(t) = 0, \alpha_1(t) \leq \beta_1(t) \\ \beta_1(t) & \text{otherwise} \end{cases}$$

In what follows, we extend the SFM to include the aforementioned delay which depends on when a flow burst actually joins the downstream queue, an event that we need to carefully specify. While a flow burst is in transit between nodes 1 and 2, let $x_{12}(t)$ be its size, i.e., the flow volume in transit before it joins $x_2(t)$. For simplicity, we assume that each flow burst is maintained during this process (i.e., the burst may not be separated in two or more sub-bursts). We will use L to denote the physical distance between nodes 1 and 2.

Predicting the time when the first flow burst actually joins queue 2 is complicated by the fact that $x_2(t)$ evolves while this burst is in transit. This is illustrated through the example in Fig. 2 which we will use to describe the evaluation of this time through a sequence of events denoted by $\{J_1, \dots, J_K\}$ with associated event times $\{\sigma_1, \dots, \sigma_K\}$. We define J_0 to be the event when the flow burst leaves node 1, i.e., the occurrence of a switch from $G_1(t^-) = 0$ to $G_1(t) = 1$, and let σ_0 be its associated occurrence time. Therefore, an estimate of the time when the flow burst joins the tail of queue 2 is given by $\sigma_1 = \sigma_0 + [L - x_2(\sigma_0)]/v(\sigma_0)$ where $v(\sigma_0)$ is the ‘‘speed’’ of the

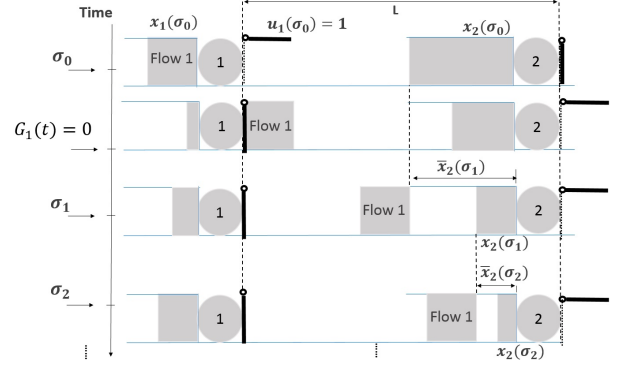


Fig. 2. Typical evolution of a flow burst in transit.

flow burst which we assume to be constant and, for notational simplicity, set it to $v(\sigma_0) = 1$ (it will become clear in the sequel that this can be relaxed and treated as random in the context of IPA). Thus, we define J_1 to be the event at time σ_1 when the flow burst covers the distance $L - x_2(\sigma_0)$. In general, however, $x_2(\sigma_1) \leq x_2(\sigma_0) \equiv \bar{x}_2(\sigma_1)$, i.e., the *estimate* $\bar{x}_2(\sigma_1)$ of $x_2(\sigma_1)$ is based on the assumption that $x_2(t)$ remains unchanged over (σ_0, σ_1) . This is illustrated in the example of Fig. 2, where $\dot{x}_2(t) = -\beta_2(t) < 0$ for some $t \in (\sigma_0, \sigma_1)$. Thus, unless $x_2(\sigma_1) = x_2(\sigma_0)$, we repeat at $t = \sigma_1$ the same process of estimating the time of the next opportunity that the flow burst might join queue 2 at time σ_2 to cover the distance $\bar{x}_2(\sigma_1) - x_2(\sigma_1)$ and define this potential *joining event* as J_2 . This process continues until event J_K occurs at time σ_K , the last event in the sequence $\{J_1, \dots, J_K\}$ when $\bar{x}_2(\sigma_K) = x_2(\sigma_K)$. Note that J_K may occur either when (i) $\bar{x}_2(\sigma_K) = x_2(\sigma_K) > 0$, in which case the estimate $\bar{x}_2(\sigma_K)$ incurs no error because $x_2(\sigma_K) = x_2(\sigma_{K-1})$, i.e., the queue length at node 2 remained unchanged because $\beta_2(t) = 0$ for $t \in [\sigma_{K-1}, \sigma_K]$, or (ii) $\bar{x}_2(\sigma_K) = x_2(\sigma_K) = 0$, in which case the flow burst joins node 2 while this queue is empty. Since in practice the queues and flow bursts may consist of discrete entities (e.g., vehicles), we define event J_K as occurring when $\bar{x}_2(t) - x_2(t) \leq \varepsilon$ for some predefined fixed small ε , i.e., a flow burst joins the downstream queue whenever it is sufficiently close to it. The following lemma asserts that the event time sequence $\{\sigma_1, \dots, \sigma_K\}$ is finite.

Lemma 1. Under the assumption that J_K is defined through $\bar{x}_2(\sigma_K) - x_2(\sigma_K) \leq \varepsilon$, the number of events K in $\{J_1, \dots, J_K\}$ is bounded. Moreover, its event time σ_K is also bounded.

Proof: Observe that $x_2(t) \leq L$, since the content of queue 2 is limited by the physical distance L . In addition, $\bar{x}_2(t) - x_2(t) > \varepsilon$ prior to event J_K . It follows that $K \leq L/\varepsilon$. Moreover, in the worst case, a flow burst travels the finite distance L to find $x_2(\sigma_K) = 0$, therefore, $\sigma_K \leq \sigma_0 + L - x_2(\sigma_0)$. ■

We now formalize the dynamics of the flow transit process described above. First, the dynamics of $\bar{x}_2(t)$, the estimated queue length when an event J_k occurs, are given by

$$\dot{\bar{x}}_2(t) = 0 \quad (4)$$

$$\bar{x}_2(t^+) = x_2(t) \quad \text{if } t = \sigma_k, k = 1, \dots, K.$$

with $\bar{x}_2(\sigma_1) = L - x_2(\sigma_0)$ and σ_0 defined above as the occurrence time of a switch from $G_1(t^-) = 0$ to $G_1(t) = 1$. The dynamics of $x_{12}(t)$ are given by

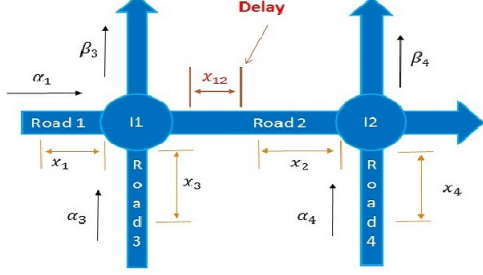


Fig. 4. Two traffic intersections.

2. Γ_i : $\alpha_i(t) - \beta_i(t)$ switches from ≤ 0 to > 0 .
3. J_k : $z_{12}(t) = \tau(\delta_{12}(t))$ representing a potential joining of the flow burst $x_{12}(t)$ with $x_2(t)$ if $\delta_{12}(t^+) > 0$, or the actual joining if $\delta_{12}(t^+) = 0$.
4. $C2O_i$: $G_i(t)$ switches from 1 to 0.
5. $O2C_i$: $G_i(t)$ switches from 0 to 1.

We can now identify the event set that affects the dynamics of the three queue content processes:

$$\Phi_1 = \{S_i, E_i, O2C_i, C2O_i\},$$

$$\Phi_2 = \{S_2, E_2, O2C_2, C2O_2, J_k\}, \quad \Phi_{12} = \{S_{12}, E_{12}, E_1, C2O_1, J_k\}$$

Finally, note that this SFM model can be extended to any network of queues with possible delays by identifying queues with dynamics of type (1) or (6) or (5).

3 MULTI-INTERSECTION TRAFFIC LIGHT CONTROL WITH DELAYS

An application of the SFM with delays arises in the Traffic Light Control (TLC) problem in transportation networks, which consists of adjusting green and red signal settings in order to control the traffic flow through an intersection and, more generally, through a set of intersections and traffic lights in an urban roadway network. The ultimate objective is to minimize congestion in an area consisting of multiple intersections. Many methods have been proposed to solve the TLC problem, including expert systems, genetic algorithms, reinforcement learning and several optimization techniques; a more detailed review of such methods may be found in Fleck et al. [2016]. Perturbation analysis methods were used in Head et al. [1996] and Fu and Howell [2003]. IPA was used in Panayiotou et al. [2005] and Geng and Cassandras [2012] for a single intersection and extended to multiple intersections in Geng and Cassandras [2015] and to quasi-dynamic control schemes in Fleck et al. [2016]. However, all this work to date has assumed that vehicles moving from one intersection to the next experience no delay. In this section, we formulate the TLC problem by including delays as in Section 2 and derive an IPA-based controller to optimize selected performance metrics (cost functions). By including delays, we will see that we can define new metrics which capture ‘‘congestion’’ in traffic systems much more accurately. As in Section 2, let $\{\alpha_i(t)\}$ and $\{\beta_i(t)\}$, $i = 1, \dots, 4$, be the incoming and outgoing flow processes respectively at all four roads shown in Fig. 4, where we now interpret $\alpha_i(t)$ as the random instantaneous vehicle arrival rate at time t . We define the controllable parameters θ_i to be the durations of the GREEN light for road $i = 1, \dots, 4$. Thus, the state vector is $x(\theta, t) = [x_1(\theta, t), x_2(\theta, t), x_3(\theta, t), x_4(\theta, t), x_{12}(\theta, t)]$ where $x_i(\theta, t)$ is the content of queue i and $x_{12}(\theta, t)$ is the content of

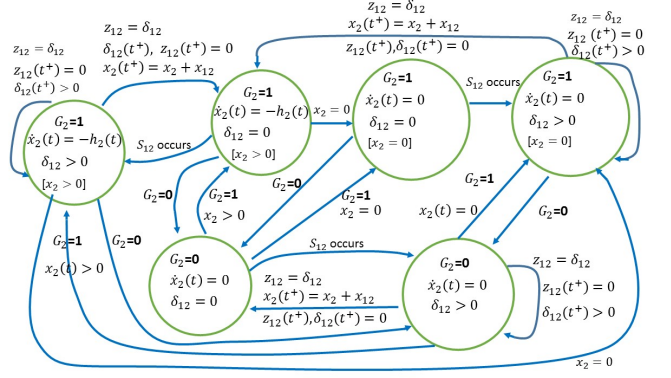


Fig. 5. Stochastic Hybrid Automaton model for $x_2(t)$.

the road between intersections $I1$ and $I2$. To maintain notational simplicity, we will assume in our analysis that **(A1)** There is no more than one traffic burst in queue 12 at any one time, **(A2)** The speed of a traffic burst $v_1(t)$ between intersections is constant, and **(A3)** There is no traffic coupling between $I1$ and $I2$. Assumptions **(A1)** and **(A2)** simplify the analysis and can be easily relaxed since our model can deal with multiple flow bursts as shown in Section 2. Assumption **(A3)** means that the distance between $I2$ and $I1$ is sufficiently large and is also made to simplify the model; it can be relaxed along the lines of Geng and Cassandras [2015].

We define clock state variables $z_i(t)$, $i = 1, \dots, 4$, which are associated with the GREEN light cycle for queue i based on (3) where the controller $G_i(t)$ is now the traffic light state, i.e., $G_i(t) = 0$ means that the traffic light in road i is RED, otherwise, it is GREEN. Accordingly, the departure rates and the queue content dynamics $x_i(t)$, $i = 1, \dots, 4$, are given by (1)-(6).

In order to provide the dynamics of $x_2(t)$ and $x_{12}(t)$, we will make use of our analysis in Section 2. In particular, let σ_0 be the time when a positive traffic flow is generated from queue 1 and enters queue 12, i.e., the light turns from RED to GREEN for road 1 and $x_1(\sigma_0) > 0$. Invoking (8), we define $\delta_{12}(t)$ to be the distance between the head of the ‘‘transit queue’’ 12 and the tail of queue 2. Thus, $\delta_{12}(\sigma_0^+) = L - x_2(\sigma_0)$. We also associate a clock to this queue, denoted by $z_{12}(t)$, which is defined by (7) and initialized at $z_{12}(\sigma_0) = 0$. Finally, $\tau(\delta_{12}(t))$ in (7) in the TLC context is given by $\tau(\delta_{12}(t)) = \delta_{12}(t)/v_1$.

Recall that a J_k event represents a *potential* joining of the flow burst from $I1$ with queue 2. The *actual* joining event occurs when $\delta_{12}(t^+) = 0$ from its initial value $\delta_{12}(\sigma_0^+) = L - x_2(\sigma_0)$. Adapting (8) and (4) to the TLC setting we get the dynamics of δ_{12} and $\bar{x}_2(t)$, while the dynamics of $x_2(t)$ and $x_{12}(t)$ are given by (6) and (5) respectively.

SFM Events. We apply the event set defined in Section 2 where we use $G2R_i$ (traffic light i changes from GREEN to RED) to replace $C2O_i$ and $R2G_i$ to replace $O2C_i$. Figure 5 shows the hybrid automaton model for queue 2 in terms of its six possible modes depending on $x_2(t)$, $G_2(t)$ and $\delta_{12}(t)$. Similar models apply to the remaining processes, all of which are generally interdependent (e.g., in Fig.5, some reset conditions involve $x_{12}(t)$).

Cost Functions. The objective of the TLC problem is to control the green cycle parameters θ_i , $i = 1, \dots, 4$, so as to minimize traffic congestion in the region covered by the two intersections

in Fig. 4. In Geng and Cassandras [2012] and Fleck et al. [2016], the average total weighted queue lengths over a fixed time interval $[0, T]$ is used to capture congestion:

$$F(\theta; x(0), z(0), T) = \frac{1}{T} \sum_{i=1}^5 \int_0^T w_i x_i(\theta, t) dt. \quad (13)$$

where w_i is the weight associated with queue i . For convenience, we will refer to (13) as the *average queue cost function*; with a slight abuse of notation we have re-indexed $x_{12}(t)$ as $x_5(t)$. However, this may not be an adequate measure of ‘‘congestion’’. For instance, it is possible that the average queue lengths over $[0, T]$ are relatively small, while reaching large values over small intervals (peak periods during a typical day). Thus, instead of restricting ourselves to (13), we define next two new cost functions.

1. Average weighted P th power of the queue lengths over a fixed interval $[0, T]$, where $P > 1$. The sample function is

$$F(\theta; x(0), z(0), T) = \frac{1}{T} \sum_{i=1}^5 \int_0^T w_i x_i^P(\theta, t) dt.$$

Observing that $x_i(\theta, t) = 0$ during an EP of queue i , we can rewrite this as

$$F(\theta; x(0), z(0), T) = \frac{1}{T} \sum_{i=1}^5 \sum_{m=1}^{M_i} \int_{\xi_{i,m}}^{\eta_{i,m}} w_i x_i^P(\theta, t) dt, \quad (14)$$

in which M_i is the total number of NEPs of queue i over a time interval $[0, T]$ and $\xi_{i,m}$, $\eta_{i,m}$ are the occurrence times of the m th S_i event and E_i event respectively. We also define the cost incurred within the m th NEP of queue i as

$$F_{i,m}(\theta) = \int_{\xi_{i,m}}^{\eta_{i,m}} w_i x_i^P(\theta, t) dt. \quad (15)$$

Clearly, when $P = 1$, (14) is reduced to (13). When $P > 1$, (14) amplifies the presence of intervals where queue lengths are large. Therefore, minimizing (14) decreases the probability that a road develops a large queue length. We will refer to this metric (14) as the *power cost function*.

2. Average weighted fraction of time that queue lengths exceed given thresholds over a fixed interval $[0, T]$. The sample function is

$$\begin{aligned} F(\theta; x(0), z(0), T) &= \frac{1}{T} \sum_{i=1}^5 \int_0^T w_i \mathbf{1}[x_i(\theta, t) > \zeta_i] dt \quad (16) \\ &= \frac{1}{T} \sum_{i=1}^5 \int_0^T w_i r_i(\theta, t) dt \end{aligned}$$

where ζ_i is a given threshold and $r_i(\theta, t) = \mathbf{1}[x_i(\theta, t) > \zeta_i]$. This necessitates the definition of two additional events: Z_i is the event such that $x_i(\theta, t) = \zeta_i$, $x_i(\theta, t^-) < \zeta_i$ (i.e., the queue content reaches the threshold from below) and \bar{Z}_i is the event such that $x_i(\theta, t) < \zeta_i$, $x_i(\theta, t^-) = \zeta_i$. Observe that $\dot{r}_i(\theta, t) = 0$ with a reset condition $r_i(\theta, t^+) = 1$ if $x_i(\theta, t^-) < \zeta_i$, $x_i(\theta, t^+) = \zeta_i$ and $r_i(\theta, t^+) = 0$ if $x_i(\theta, t^-) = \zeta_i$, $x_i(\theta, t^+) < \zeta_i$. Finally, we use $F_{i,m}(\theta)$ as in (15), for the cost associated with the m th NEP at queue i :

$$F_{i,m}(\theta) = \int_{\gamma_{i,m}(\theta)}^{\psi_{i,m}(\theta)} w_i r_i(\theta, t) dt. \quad (17)$$

where $\gamma_{i,m}$, $\psi_{i,m}$ are the start and end respectively of an interval such that $r_i(\theta, t) = 1$.

Optimization. Our purpose is to minimize the cost functions defined in (13), (14) and (16). We define the overall cost function as follows:

$$H(\theta; x(0), z(0), T) = E[F(\theta; x(0), z(0), T)],$$

in which $F(\theta; x(0), z(0), T)$ is a sample cost function of the form (13), (14) or (16). Clearly, we cannot derive a closed-form expression for the expectation above. However, we can estimate the gradient $\nabla H(\theta)$ through the sample gradient $\nabla F(\theta)$ based on IPA, which has been shown to be unbiased under mild technical conditions (Proposition 1 in Cassandras et al. [2010]). We emphasize that *no explicit knowledge of $\alpha_i(t)$ and $h_i(t)$ is necessary* to estimate $\nabla H(\theta)$. The IPA estimators derived in the next section only need estimates of $\alpha_i(\tau_k)$ and $h_i(\tau_k)$ at certain event times τ_k . Using $\nabla F(\theta)$, we can use a simple gradient-descent optimization algorithm to minimize the associated cost metric through the iterative scheme

$$\theta_{j,k+1} = \theta_{j,k} - c_k Q_{j,k}(\theta_k, x(0), T, \omega_k),$$

in which $Q_{j,k}(\theta_k, x(0), T, \omega_k)$ is an estimator of $dH/d\theta_j$ (in our case, $dF/d\theta_j$) in sample path ω_k and c_k is the step size at the k th iteration selected through an appropriate decreasing sequence to guarantee convergence (Fleck et al. [2016]). In the next section, we use the IPA methodology to obtain $dF/d\theta_j$ through the state derivatives $\frac{\partial x_i(\theta, t)}{\partial \theta_j}$.

4 INFINITESIMAL PERTURBATION ANALYSIS (IPA)

We briefly review the IPA framework for general stochastic hybrid systems as presented in Cassandras et al. [2010]. Let $\{\tau_k(\theta)\}$, $k = 1, \dots, K$, denote the occurrence times of all events in the state trajectory of a hybrid system with dynamics $\dot{x} = f(x, \theta, t)$ over an interval $[\tau_k(\theta), \tau_{k+1}(\theta))$, where $\theta \in \Theta$ is some parameter vector and Θ is a given compact, convex set. For convenience, we set $\tau_0 = 0$ and $\tau_{K+1} = T$. We use the Jacobian matrix notation: $x'(t) \equiv \frac{\partial x(\theta, t)}{\partial \theta}$ and $\tau'_k \equiv \frac{\partial \tau_k(\theta)}{\partial \theta}$, for all state and event time derivatives. It is shown in Cassandras et al. [2010] that

$$\frac{d}{dt} x'(t) = \frac{\partial f_k(t)}{\partial x} x'(t) + \frac{\partial f_k(t)}{\partial \theta}, \quad (18)$$

for $t \in [\tau_k, \tau_{k+1})$ with boundary condition:

$$x'(\tau_k^+) = x'(\tau_k^-) + [f_{k-1}(\tau_k^-) - f_k(\tau_k^+)] \tau'_k \quad (19)$$

for $k = 1, \dots, K$. In order to complete the evaluation of $x'(\tau_k^+)$ in (19), we need to determine τ'_k . If the event at τ_k is *exogenous* (i.e., independent of θ), $\tau'_k = 0$. However, if the event is *endogenous*, there exists a continuously differentiable function $g_k : \mathbb{R}^n \times \Theta \rightarrow \mathbb{R}$ such that $\tau_k = \min\{t > \tau_{k-1} : g_k(x(\theta, t), \theta) = 0\}$ and, as long as $\frac{\partial g_k}{\partial x} f_k(\tau_k^-) \neq 0$,

$$\tau'_k = - \left[\frac{\partial g_k}{\partial x} f_k(\tau_k^-) \right]^{-1} \left[\frac{\partial g_k}{\partial \theta} + \frac{\partial g_k}{\partial x} x'(\tau_k^-) \right] \quad (20)$$

In our TLC setting, we will use the notation

$$x'_{i,j}(t) = \frac{\partial x_i(\theta, t)}{\partial \theta_j}, z'_{i,j}(t) = \frac{\partial z_i(\theta, t)}{\partial \theta_j}, \tau'_{k,j}(t) = \frac{\partial \tau_k(\theta)}{\partial \theta_j}$$

We also note that in (1),(5), $\frac{\partial f_k(t)}{\partial \theta} = \frac{\partial f_k(t)}{\partial x} = 0$ and (18) reduces to

$$\dot{x}'_{i,j}(t) = \dot{x}'_{i,j}(\tau_k^+), \quad t \in (\tau_k, \tau_{k+1}] \quad (21)$$

4.1 State and Event Time Derivatives

We will now apply the IPA equations (19)-(21) to our TLC setting on an event by event basis for each of the events sets Φ_i , $i = 1, \dots, 4$, and Φ_{12} . In all cases, τ_k denotes the associated event time.

4.1.1 IPA for Event Set $\Phi_i = \{S_i, E_i, R2G_i, G2R_i\} \cup \{Z_i, \bar{Z}_i\}$, $i = 1, 3, 4$ IPA for these three processes for each of the events in the first set above is identical to that in Geng and Cassandras [2012]. Thus, we simply summarize the results here.

(1) Event E_i : $x'_{i,j}(\tau_k^+) = 0$.

(2) Event $G2R_i$: Let ρ_k be the time of the last $R2G_i$ event before $G2R_i$ occurs. Then, $\tau'_{k,j} = \mathbf{1}[j = i] + \rho'_{k,j}$ and

$$x'_{i,j}(\tau_k^+) = \begin{cases} x'_{i,j}(\tau_k) - \alpha_i(\tau_k)\tau'_{k,j} & \text{if } x_i(t) = 0, \alpha_i(t) \leq \beta_i(t) \\ x'_{i,j}(\tau_k) - h_i(\tau_k)\tau'_{k,j} & \text{otherwise} \end{cases} \quad (22)$$

(3) Event $R2G_i$: Let ρ_k be the time of this event and τ_k be the time of the last $G2R_i$ event before $R2G_i$ occurs. We will use the notation \bar{i} to denote the index of a road perpendicular to i (e.g., $\bar{1} = 3, \bar{2} = 4$). Then, $\rho'_{k,j} = \mathbf{1}[j = \bar{i}] + \tau'_{k,j}$ and

$$x'_{i,j}(\rho_k^+) = \begin{cases} x'_{i,j}(\rho_k) + \alpha_i(\rho_k)\rho'_{k,j} & \text{if } x_i(t) = 0, \alpha_i(t) \leq \beta_i(t) \\ x'_{i,j}(\rho_k) + h_i(\rho_k)\rho'_{k,j} & \text{otherwise} \end{cases} \quad (23)$$

(4) Event S_i : If S_i is induced by $G2R_i$, then $x'_{i,j}(\tau_k^+) = x'_{i,j}(\tau_k) - \alpha_i(\tau_k)\tau'_{k,j}$. If S_i is an exogenous event triggered by Γ_i , then $x'_{12,j}(\tau_k^+) = x'_{12,j}(\tau_k)$.

For the two new events $\{Z_i, \bar{Z}_i\}$, we have:

(5) Event Z_i : This is an endogenous event which occurs when $g_k(x(\theta, t), \theta) = x_i(\tau_k) - \zeta_i = 0$. Applying (20), we have

$$\tau'_{k,j} = \begin{cases} -x'_{i,j}(\tau_k)/\alpha_i(\tau_k) & \text{if } G_i(t) = 0 \\ -x'_{i,j}(\tau_k)/[\alpha_i(\tau_k) - h_i(\tau_k)] & \text{if } G_i(t) = 1 \end{cases} \quad (24)$$

Moreover, based on the definition $r_i(t) = \mathbf{1}[x_i(t) > \zeta_i]$ in Section 3, $r_i(\tau_k^+) = 1$, which implies that $r'_{i,j}(\tau_k^+) + \dot{r}(\tau_k^+)\tau'_{k,j} = 0$. Since $\dot{r}_i(\tau_k^+) = 0$, we get $r'_{i,j}(\tau_k^+) = 0$.

(6) Event \bar{Z}_i : Similar to the previous case, $g_k(x(\theta, t), \theta) = x_i(\tau_k) - \zeta_i = 0$ and applying (20) gives

$$\tau'_{k,j} = -x'_{i,j}(\tau_k)/(\alpha_i(\tau_k) - h_i(\tau_k)) \quad (25)$$

In this case, $r_i(\tau_k^+) \equiv 0$, therefore, $r'_{i,j}(\tau_k^+) + \dot{r}_i(\tau_k^+)\tau'_{k,j} = 0$ and, since $\dot{r}_i(\tau_k^+) = 0$, we get $r'_{i,j}(\tau_k^+) = 0$.

4.1.2 IPA for Event Set $\Phi_2 = \{S_2, E_2, R2G_2, G2R_2, J_k\} \cup \{Z_2, \bar{Z}_2\}$ IPA for this set and for Φ_{12} is different as detailed next.

(1) Event E_2 : This is an endogenous event ending an EP that occurs when $g_k(x(\theta, t), \theta) = x_2(t) = 0$ at $t = \tau_k$. Applying (20) and using (6), we have $\tau'_{k,j} = x'_{2,j}(\tau_k^-)/h_2(\tau_k^-)$. It then follows from (19) that $x'_{2,j}(\tau_k^+) = x'_{2,j}(\tau_k^-) - h_2(\tau_k^-)\tau'_{k,j} = 0$.

(2) Event S_2 : In view of the reset condition in (6), this event is induced by J_k provided $\delta_{12}(t^+) = 0$. As described in Section 2, a sequence of J_k events is initiated when a flow burst is generated at node 1 with associated event times $\{\sigma_0, \sigma_1, \dots, \sigma_K\}$. Event S_2 is induced by the last occurrence of a J_k event at time σ_K . Thus, our goal here is to evaluate the IPA derivative $x'_{2,j}(\sigma_K^+)$. At first sight, it would appear that this requires the complete sequence $\{x'_{2,j}(\sigma_0^+), \dots, x'_{2,j}(\sigma_{K-1}^+)\}$ along with event

time derivatives $\{\sigma'_{0,j}, \dots, \sigma'_{K-1,j}\}$ from which $x'_{2,j}(\sigma_K^+)$ can be inferred. However, the following lemma shows that the only information needed from the full sequence of J_k events is σ'_0 .

Lemma 2. Let σ_k , $k = 0, 1, \dots, K$ be the occurrence time of event J_k for a flow burst initiated at σ_0 . Then,

$$\sigma'_{k,j} = \frac{-1}{v_1} [x'_{2,j}(\sigma_{k-1}) + \dot{x}_2(\sigma_{k-1})\sigma'_{k-1,j}] + \sigma'_{0,j}$$

Proof: Event J_k at $t = \sigma_k$ is endogenous and occurs when $g_k(x(\theta, \sigma_k), \theta) = z_{12}(\sigma_k) - \delta_{12}(\sigma_k)/v_1 = 0$. Applying (20) and using (7),(8), we get $\sigma'_{k,j} = \delta'_{12,j}(\sigma_k)/v_1 - z'_{12,j}(\sigma_k)$. Using (21), we have $\delta'_{12,j}(\sigma_k) = \delta'_{12,j}(\sigma_{k-1}^+)$ and it follows that

$$\sigma'_{k,j} = \delta'_{12,j}(\sigma_{k-1}^+)/v_1 - z'_{12,j}(\sigma_k) \quad (26)$$

Again applying (21) gives $z'_{12,j}(\sigma_k) = z'_{12,j}(\sigma_{k-1}^+)$. From (19), in view of (7), we get, for $k = 1$, $z'_{12,j}(\sigma_0^+) = -\sigma'_{0,j}$. The reset condition in (8) implies that $\delta_{12}(\sigma_0^+) = L - x_2(\sigma_0)$, hence $\delta'_{12,j}(\sigma_0^+) = -x'_{2,j}(\sigma_0) - \dot{x}_2(\sigma_0)\sigma'_{0,j}$. Thus, in this case, (26) gives:

$$\sigma'_{1,j} = \frac{-1}{v_1} [x'_{2,j}(\sigma_0) + \dot{x}_2(\sigma_0)\sigma'_{0,j}] + \sigma'_{0,j} \quad (27)$$

For $k > 1$, based on the reset condition in (7), we have $z_{12}(\sigma_k^+) = 0$. Taking the total derivative, we get $z'_{12,j}(\sigma_k^+) = -\sigma'_{k,j}$. The reset condition in (8) now implies that $\delta_{12}(\sigma_{k-1}^+) = \bar{x}_2(\sigma_{k-1}) - x_2(\sigma_{k-1})$, hence

$$\delta'_{12,j}(\sigma_{k-1}^+) = \bar{x}'_{2,j}(\sigma_{k-1}) + \dot{\bar{x}}_2(\sigma_{k-1})\sigma'_{k-1,j} - x'_{2,j}(\sigma_{k-1}) - \dot{x}_2(\sigma_{k-1})\sigma'_{k-1,j} \quad (28)$$

Applying (21), we have $\bar{x}'_{2,j}(\sigma_{k-1}) = \bar{x}'_{2,j}(\sigma_{k-2}^+)$. Looking at (4), we have $\dot{\bar{x}}_2(\sigma_{k-1}) = 0$ and the reset condition implies that $\bar{x}'_{2,j}(\sigma_{k-2}^+) = x'_{2,j}(\sigma_{k-2}) + \dot{x}_2(\sigma_{k-2})\sigma'_{k-2,j}$. Thus, returning to (28), we get

$$\delta'_{12,j}(\sigma_{k-1}^+) = x'_{2,j}(\sigma_{k-2}) + \dot{x}_2(\sigma_{k-2})\sigma'_{k-2,j} - x'_{2,j}(\sigma_{k-1}) - \dot{x}_2(\sigma_{k-1})\sigma'_{k-1,j} \quad (29)$$

Recalling that $z'_{12,j}(\sigma_k^+) = -\sigma'_{k,j}$ and combining (27),(29) into (26), we get

$$\begin{aligned} \sigma'_{k,j} &= \sigma'_{k-1,j} + \frac{1}{v_1} [x'_{2,j}(\sigma_{k-2}) + \dot{x}_2(\sigma_{k-2})\sigma'_{k-2,j} \\ &\quad - x'_{2,j}(\sigma_{k-1}) - \dot{x}_2(\sigma_{k-1})\sigma'_{k-1,j}] \\ &= \sigma'_{0,j} + \frac{1}{v_1} [-x'_{2,j}(\sigma_{k-1}) - \dot{x}_2(\sigma_{k-1})\sigma'_{k-1,j}] \end{aligned} \quad (30)$$

where the last step follows from a recursive evaluation of $\sigma'_{k-1,j}$ using (27) and (30) leading to many of the terms above canceling. This completes the proof. ■

Let us now focus on event J_K at time σ_K . It follows from the reset condition in (6) that

$$x'_{2,j}(\sigma_K^+) = \begin{cases} x'_{2,j}(\sigma_K) + x'_{12,j}(\sigma_K) & \text{if } G_2(\sigma_K) = 1 \\ +h_2(\sigma_K^+)\sigma'_{K,j} & \text{and } x_2(\sigma_K) = 0 \\ x'_{2,j}(\sigma_K) + x'_{12,j}(\sigma_K) & \text{otherwise} \end{cases} \quad (31)$$

Recall that $\delta_{12}(\sigma_K^+) = 0$ in (31). If $G_2(\sigma_K) = 1$ and $x_2(\sigma_K) = 0$, then $x_2(\sigma_{K-1}) - x_2(\sigma_K) = 0$, hence $x_2(\sigma_{K-1}) = 0$. It follows from (6) and (8) that $\dot{x}_2(\sigma_{K-1}) = 0$. Based on Case 1 above, we get $x'_{2,j}(\sigma_{K-1}) = 0$. Then, from Lemma 2, $\sigma'_{K,j} = \sigma'_{0,j}$ and (31) becomes

$$x'_{2,j}(\sigma_K^+) = \begin{cases} x'_{2,j}(\sigma_K) + x'_{12,j}(\sigma_K) & \text{if } G_2(\sigma_K) = 1 \\ +h_2(\sigma_K^+) \sigma'_{0,j} & \text{and } x_2(\sigma_K) = 0. \\ x'_{2,j}(\sigma_K) + x'_{12,j}(\sigma_K) & \text{otherwise} \end{cases} \quad (32)$$

We conclude that the state derivative $x'_{2,j}(\sigma_K^+)$ when event S_2 occurs is independent of all event time derivatives $\sigma'_{1,j}, \dots, \sigma'_{K,j}$ and involves only $\sigma'_{0,j}$, evaluated when the associated flow burst is initiated.

(3) Event $G2R_2$: This is an endogenous event that occurs when $g_k(x(\theta, t), \theta) = z_2(t) - \theta_2 = 0$. Based on (20), $\tau'_{k,j} = \mathbf{1}[j = 2] - z'_{2,j}(\tau_k)$. Let ρ_k be the last $R2G_2$ before $G2R_2$ occurs. Applying (21), we have $z'_{2,j}(\rho_k^+) = z'_{2,j}(\tau_k)$. and from (19) we get $z'_{2,j}(\rho_k^+) = -\rho'_{k,j}$. It follows that $\tau'_{k,j} = \mathbf{1}[j = 2] + \rho'_{k,j}$. Based on (19), we have

$$x'_{2,j}(\tau_k^+) = \begin{cases} x'_{2,j}(\tau_k) - h_2(\tau_k) \tau'_{k,j} & \text{if } x_2(\tau_k) > 0 \\ x'_{2,j}(\tau_k) & \text{otherwise} \end{cases} \quad (33)$$

(4) Event $R2G_2$: Let ρ_k be the time of this event and τ_k be the time of the last $G2R_2$ event before $R2G_2$ occurs. Similar to (3) above, we get $\rho'_{k,j} = \mathbf{1}[j = 4] + \tau'_{k,j}$ and use this value in the expression below which follows from (19):

$$x'_{2,j}(\rho_k^+) = \begin{cases} x'_{2,j}(\rho_k) + h_2(\tau_k^+) \rho'_{k,j} & \text{if } x_2(\rho_k) > 0 \\ x'_{2,j}(\rho_k) & \text{otherwise} \end{cases} \quad (34)$$

(5) Event J_k : The analysis of this event has already been done in Case (2) above, including Lemma 2.

(6) Event Z_2 : This is an endogenous event which is triggered by J_k : if a traffic burst from node 1 joins $x_2(t)$ at $t = \tau_k$ and $x_2(\tau_k^+) > \zeta_2$, this results in Z_2 . Since $r_2(\tau_k^+) = 1$ and $\dot{r}_2(t) = 0$, we have $r'_{2,j}(\tau_k^+) = 0$.

(7) Event \bar{Z}_2 : This is an endogenous event that occurs when $g_k(x(\theta, t), \theta) = x_2(\theta, t) - \zeta_2 = 0$. Applying (20), we have $\tau'_{k,j} = x'_2(\tau_k)/h_2(\tau_k)$. Moreover, $r_2(\tau_k^+) \equiv 0$, therefore, $r'_{2,j}(\tau_k^+) + \dot{r}_2(\tau_k^+) \tau_k^+ = 0$ and, since $\dot{r}_2(\tau_k^+) = 0$, we get $r'_{2,j}(\tau_k^+) = 0$.

4.1.3 IPA for Event Set $\Phi_{12} = \{S_{12}, E_{12}, E_1, G2R_1, J_k\} \cup \{Z_{12}, \bar{Z}_{12}\}$

(1) Event S_{12} : This event can be either exogenous or endogenous. If $x_1(\tau_k) > 0$ or if $x_1(\tau_k) = 0, \alpha_1(t) > 0$, S_{12} is induced by event $R2G_1$ which is endogenous. Otherwise, S_{12} is exogenous event and occurs when $G_1(\tau_k) = 1$ and $\alpha_1(\tau_k)$ switches from zero to some positive value.

Case (1a): S_{12} is induced by $R2G_1$. Referring to our analysis of $R2G_1$ (Case (3) for Φ_1), we have already evaluated $\tau'_{k,j}$. Then, applying (19), we get

$$x'_{12,j}(\tau_k^+) = \begin{cases} x'_{12,j}(\tau_k) - \alpha_1(\tau_k^+) \tau'_{k,j} & \text{if } x_1(\tau_k) = 0 \text{ and} \\ x'_{12,j}(\tau_k) - h_1(\tau_k^+) \tau'_{k,j} & 0 < \alpha_1(\tau_k) \leq \beta_1(\tau_k). \\ x'_{12,j}(\tau_k) & \text{otherwise} \end{cases} \quad (35)$$

Case(1b) S_{12} is exogenous. In this case, $\tau'_{k,j} = 0$ and applying (19) gives $x'_{12,j}(\tau_k^+) = x'_{12,j}(\tau_k)$.

(2) Event E_{12} : This event occurs when the traffic burst in queue 12 joins queue 2. This is an endogenous event that occurs when

$g_k(x(\theta, \tau_k), \theta) = z_{12}(\tau_k) - \delta_{12}(\tau_k) = 0$ and $\delta_{12}(\tau_k^+) = 0$. When this happens, it follows from the reset condition in (5) that $x'_{12,j}(\tau_k^+) = 0$.

(3) Event E_1 : This is an endogenous event that occurs when $g_k(x(\theta, t), \theta) = x_1(t) = 0$. Applying (20), we get $\tau'_{k,j} = -\frac{x'_{1,j}(\tau_k)}{\alpha_1(\tau_k) - h_1(\tau_k)}$. Thus, using (19), we get

$$x'_{12,j}(\tau_k^+) = x'_{12,j}(\tau_k) + (h_1(\tau_k) - \alpha_1(\tau_k)) \tau'_{k,j} \\ = x'_{12,j}(\tau_k) + x'_{1,j}(\tau_k) \quad (36)$$

(4) Event $G2R_1$: This is an endogenous event that occurs when $g_k(x(\theta, t), \theta) = z_1(t) - \theta_1 = 0$. It was shown under the analysis for events in Φ_1 that for $G2R_1$ we have $\tau'_{k,j} = \mathbf{1}[j = i] + \rho'_{k,j}$ where ρ_k is the time of the last $R2G_1$ event before $G2R_1$ occurs. Using this value, we can evaluate the following which follows from (19):

$$x'_{12,j}(\tau_k^+) = \begin{cases} x'_{12,j}(\tau_k) + \alpha_1(\tau_k) \tau'_{k,j} & \text{if } x_1(\tau_k) = 0 \\ x'_{12,j}(\tau_k) + h_1(\tau_k) \tau'_{k,j} & \text{and } \alpha_1(t) \leq \beta_1(t) \\ x'_{12,j}(\tau_k) & \text{otherwise} \end{cases} \quad (37)$$

(5) Event J_k : The analysis of this event has already been done in Case (2) above, including Lemma 2.

(6) Event Z_{12} : This is an endogenous event that occurs when $g_k(x(\theta, t), \theta) = x_{12}(\theta, t) - \zeta_{12} = 0$. Applying (20), we have

$$\tau'_{k,j} = \begin{cases} -\frac{x'_{12,j}(\tau_k)}{\alpha_1(\tau_k)} & \text{if } x_1(\tau_k) = 0 \\ -\frac{x'_{12,j}(\tau_k)}{h_1(\tau_k)} & \text{and } \alpha_1(t) \leq \beta_1(t). \\ \text{otherwise} \end{cases}$$

Since $r_{12}(\tau_k^+) = 1$ and $\dot{r}_{12}(t) = 0$, we have $r'_{12,j}(\tau_k^+) = 0$.

(7) Event \bar{Z}_{12} : This is triggered by event E_{12} when the traffic burst in queue 12 joins queue 2 and we reset $x_{12}(\tau_k^+) = 0$. Since $r_{12}(\tau_k^+) = 0$ and $\dot{r}_{12}(t) = 0$, we have $r'_{12,j}(\tau_k^+) = 0$.

4.2 Cost Function Derivatives

Returning to (13), (14), and (16), recall that the IPA estimator consists of the gradient formed by the sample performance derivatives $\frac{dF}{d\theta_j}$, which in turn depend on the state derivatives that we have evaluated in the previous section. The derivation of the IPA estimator for the Average Queue cost function in (13) is similar to that in Geng and Cassandras [2012] and related prior work and is omitted. Instead, we concentrate on the two new cost functions (14), and (16).

For the Power cost function, we derive $\frac{dF_{i,m}(\theta)}{d\theta_j}$ from (15), from which $\frac{dF}{d\theta_j}$ is obtained by adding over all M_i NEPs of each queue i over $[0, T]$:

$$\begin{aligned} \frac{dF_{i,m}(\theta)}{d\theta_j} &= P x'_{i,j}(\theta, t) \int_{\xi_{i,m}(\theta)}^{\eta_{i,m}(\theta)} w_i x_i^{P-1}(\theta, t) dt \\ &= P [x'_{i,j}(\xi_{i,m}^+) \int_{\xi_{i,m}(\theta)}^{\xi_{i,m}^+} w_i x_i^{P-1}(\theta, t) dt \\ &\quad + \sum_{j=2}^{J_{i,m}} x'_{i,j}((t_{i,m}^j)^+) \int_{t_{i,m}^{j-1}}^{t_{i,m}^j} w_i x_i^{P-1}(\theta, t) dt \\ &\quad + x'_{i,j}((t_{i,m}^{J_{i,m}})^+) \int_{t_{i,m}^{J_{i,m}-1}}^{\eta_{i,m}} w_i x_i^{P-1}(\theta, t) dt], \end{aligned}$$

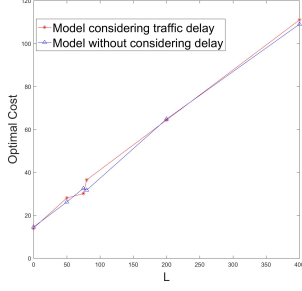


Fig. 6. Comparison of Optimal Average Queue Cost vs L.

where $t_{i,m}^j, j = 1, \dots, J_{i,m}$ is the occurrence time of the j th event in the m th NEP of queue i . The state derivative is determined on an event-driven basis using $x'_{i,j}(\tau_k^+)$ corresponding to the event occurring at time τ_k ; for instance, if $G2R_1$ occurs at node 1, then (22) is invoked with $i = 1$.

For the Threshold cost function, we know that $r'(\theta, t) = 0$ and it follows from (17):

$$\begin{aligned} \frac{dF_{i,m}(\theta)}{d\theta_j} &= \int_{\gamma_{i,m}(\theta)}^{\psi_{i,m}(\theta)} w_i r'_{i,j}(\theta, t) dt - w_i r_i(\theta, \gamma_{i,m}^+) \gamma'_{i,m,j} \\ &\quad + w_i r_i(\theta, \psi_{i,m}^-) \psi'_{i,m,j} \\ &= w_i (\psi'_{i,m,j} - \gamma'_{i,m,j}), \end{aligned}$$

Note that in this case the derivative depends only on $\psi'_{i,m,j}, \gamma'_{i,m,j}$, the event time derivatives in (24),(25) for $i = 1, 3, 4$ and the corresponding event time derivatives in Cases (6),(7) for each of sets Φ_{22} and Φ_{12} .

5 SIMULATION RESULTS

In this section, we use the derived IPA estimators in order to optimize the green light cycles in the two-intersection model of Fig. 4. We stress that this model is simulated as a Discrete Event System (DES) with individual vehicles rather than flows, so that the resulting estimators are based on actual observed data. This is made possible by the fact that all SFM events in the sets $\Phi_i, i = 1, \dots, 4$, and Φ_{12} coincide with those of the DES, therefore they are directly observable along with their occurrence times.

We assume that all vehicle arrival processes are Poisson (recall, however, that IPA is *independent of these distributions*) with rates $\bar{\alpha}_i, i = 1, 3, 4$, and that the vehicle departure rate $h_i(t)$ on each non-empty road is constant. In Geng and Cassandras [2015], only one controllable parameter per intersection was considered by setting $\theta_i + \theta_j = C$. Here, we relax this constraint. Moreover, we limit each controllable parameter so that $\theta_i \in [\theta_{i,min}, \theta_{i,max}]$. In our simulations, $\alpha_i(\tau_k)$ is estimated through N_a/t_w by counting the number of arriving vehicles N_a over a time interval $[0, t_w]$ and $h_i(t)$ is estimated using the same method as in Fleck et al. [2016]. Three sets of simulations are presented below, one for each of the three cost metrics in (13), (14) and (16).

1. Average Queue Cost Function. We minimize metric (13), over $[0, T]$. All three arrival processes are Poisson with rates $\bar{\alpha} = [0.41, 0.45, 0.32]$ and the departure rates at roads 1, 2, 3, 4 are $[1.2, 1.3, 1.2, 1.1]$. We choose $T = 1000s$, $w_i = 1$ and $\theta_i \in [10, 50]$ for all i , and the initial θ_i values are $[40, 20, 20, 40]$. Figure 6 shows the optimal cost (averaged over 10 sample paths) considering the transit delay in SFM between intersections (red

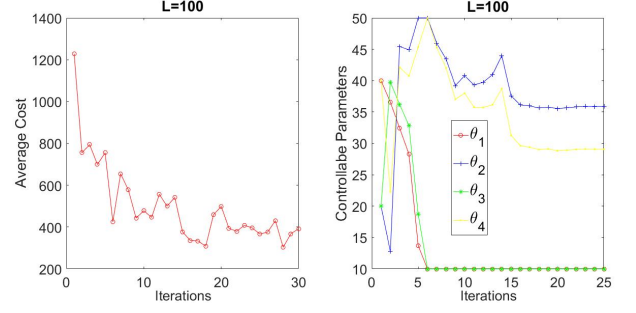


Fig. 7. Optimal Power Cost Function vs Iterations.

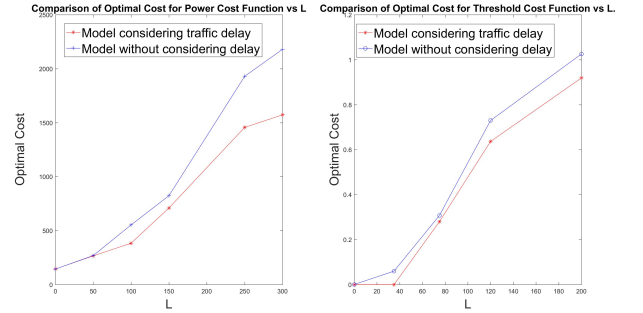


Fig. 8. Comparison of Optimal Cost with/without delay vs L.

curve) and ignoring this delay (blue curve) as a function of L. In this case, delay has no effect on the long term total average queue length, as expected. However, this metric may not accurately capture traffic congestion.

2. Power Cost Function, $P = 2$. For the same settings as before and a quadratic queuing cost, Fig. 7 shows how this cost function and the associated controllable parameters converge when $L = 100$, achieving a 40% cost decrease. In the left plot of Fig. 8, we use the SFM both including the transit delay and ignoring this delay in order to compare the optimal costs under these two models. Clearly, including delays in our IPA estimators for $L > 0$ achieves a lower cost, with the gap increasing as L increases.

3. Threshold Cost Function. For the same settings and a common threshold $\zeta_i = 25$ for all i and with $L = 35$, Fig. 9 shows how this cost function and the associate controllable parameters converge, with the cost converging to its zero lower bound, therefore, in this case we see that our approach reaches the global optimum. In the right plot of Fig. 8, we apply the SFM considering both the transit delay between intersections and ignoring this delay so as to compare the resulting optimal costs. Once again, including delays achieves a lower cost, with the gap increasing as L increases.

In Fig. 10, we provide histograms of the queue contents when $L = 35$. On the left, the controllable parameters are at their initial values $[40, 20, 20, 40]$ and we can see that queues 2, 3, and 12 frequently exceed the threshold. Under the optimal solution we obtain (right side) taking the transit delay between intersections into account, observe that no queue ever exceeds the threshold over $[0, T]$, hence the optimal cost 0 is obtained. Moreover, note that the probabilities that $x_2(t) = 0$ and $x_3(t) = 0$ significantly increase indicating a much improved traffic balance.

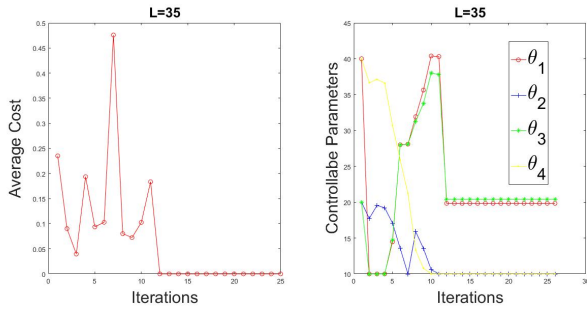


Fig. 9. Optimal Threshold Cost Function vs Iterations.

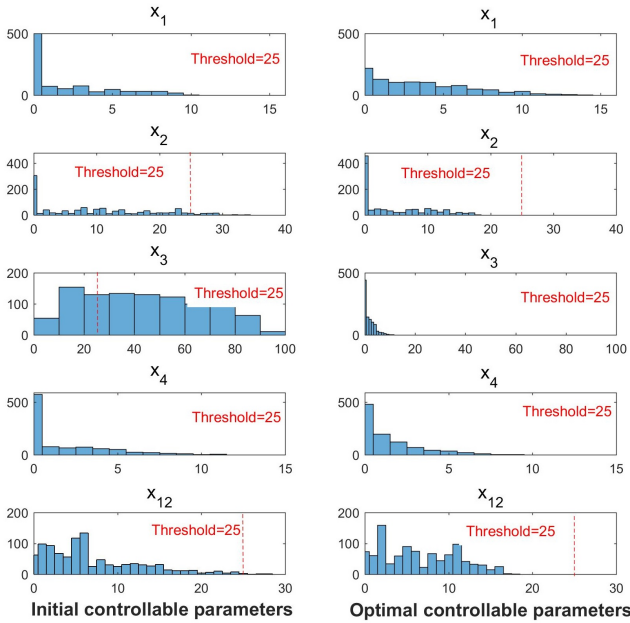


Fig. 10. Distribution of queue lengths under $L = 35$.

6 CONCLUSIONS AND FUTURE WORK

We have extended SFMs to allow for delays which can arise in the flow movement. We have applied this framework to the multi-intersection traffic light control problem by including transit delays for vehicles moving from one intersection to the next and developed IPA for this extended SFM in order to derive on-line gradient estimates of several congestion cost metrics with respect to the controllable green/red cycle lengths, including two new cost metrics that better capture congestion. Our simulation results show that the inclusion of delays in our analysis leads to improved performance relative to models that ignore delays. Future work aims at extensions to allow traffic blocking between intersections and allowing multiple traffic bursts between intersections.

References

- Anderson, M.P., Woessner, W.W., and Hunt, R.J. (2015). *Applied groundwater modeling: simulation of flow and advective transport*. Academic Press.
- Armony, M., Israelit, S., Mandelbaum, A., Marmor, Y.N., Tseytlin, Y., Yom-Tov, G.B., et al. (2015). On patient flow in hospitals: A data-based queueing-science perspective. *Stochastic Systems*, 5(1), 146–194.
- Cassandras, C.G., Wardi, Y., Melamed, B., Sun, G., and Panayiotou, C.G. (2002). Perturbation analysis for on-line

- control and optimization of stochastic fluid models. *IEEE Transactions on Automatic Control*, 47(8), 1234–1248.
- Cassandras, C.G., Wardi, Y., Panayiotou, C.G., and Yao, C. (2010). Perturbation analysis and optimization of stochastic hybrid systems. *European Journal of Control*, 6(6), 642–664.
- Cassandras, C.G. and Lafortune, S. (2009). *Introduction to discrete event systems*. Springer.
- Fleck, J.L., Cassandras, C.G., and Geng, Y. (2016). Adaptive quasi-dynamic traffic light control. *IEEE Transactions on Control Systems Technology*, 24(3), 830–842.
- Fu, M.C. and Howell, W.C. (2003). Application of perturbation analysis to traffic light signal timing. *Proc. IEEE Conf. on Decision and Control*, 4837–4840.
- Geng, Y. and Cassandras, C.G. (2012). Traffic light control using infinitesimal perturbation analysis. In *2012 IEEE 51st Annual Conf. on Decision and Control (CDC)*, 7001–7006. IEEE.
- Geng, Y. and Cassandras, C.G. (2015). Multi-intersection traffic light control with blocking. *Discrete Event Dynamic Systems*, 25(1-2), 7–30.
- Head, L., Ciarallo, F., and Kaduwela, D.L. (1996). A perturbation analysis approach to traffic signal optimization. *INFORMS National Meeting*.
- Panayiotou, C.G., Howell, W.C., and Fu, M.C. (2005). On-line traffic light control through gradient estimation using stochastic flow models. *Proc. IFAC World Congress*.
- Wardi, Y., Adams, R., and Melamed, B. (2010). A unified approach to infinitesimal perturbation analysis in stochastic flow models: the single-stage case. *IEEE Transactions on Automatic Control*, 55(1), 89–103.
- Yao, C. and Cassandras, C.G. (2011). Perturbation analysis of stochastic hybrid systems and applications to resource contention games. *Frontiers of Electrical and Electronic Engineering in China*, 6(3), 453–467.
- Yin, S., Ding, S.X., Abandan Sari, A.H., and Hao, H. (2013). Data-driven monitoring for stochastic systems and its application on batch process. *Intl. Journal of Systems Science*, 44(7), 1366–1376.